Dentistry 3000

Vol 14, No 2 (2026)
ISSN 2167-8677 (online)
DOI 10.5195/d3000/2026.1596

Histomorphometric and Temporal Evaluation of Bacterial-Induced Mandibular Bone Marrow Inflammation (Osteomyelitis)

Mustafa Basim Ali[1], Ansam Mahdi Khalel[1], Noor Mohammed Hadi Layedh[1], Ghassan N. Talib[2]
[1]*College of Dentistry, University of Kufa, Najaf, Iraq*
[2]*Collegy of Dentistry,University of Alkafeel, Najaf, Iraq*

Abstract

Bacterial osteomyelitis and isolated bone marrow inflammation of the mandible represent critical clinical challenges in dentistry. While cortical bone dynamics are well documented, early intramedullary cellular events remain poorly quantified. This study quantitatively evaluated the temporal histopathological changes and differential inflammatory cell recruitment in rat mandibular bone marrow following induced *Staphylococcus aureus* infection at 5 and 10 days post inoculation via digital histomorphometry. Twenty-four adult male Wistar rats ($200 - 250$ g) were randomly allocated into Control ($n = 12$) and Infected ($n = 12$) groups, subdivided into Day 5 and Day 10 interval endpoints ($n = 6$ per subgroup). Bacterial marrow infection was induced via intraosseous injection of 1×10^7 CFU/mL *S. aureus*. Mandibular specimens were processed, decalcified in EDTA, stained with Hematoxylin and Eosin (H&E), and quantitatively analyzed using ImageJ software. At Day 5, infected marrow exhibited a significant surge in overall cellular density ($8{,}900 \pm 620$ cells/mm^2) compared to control ($4{,}250 \pm 310$ cells/mm^2, $p < 0.001$), driven by acute neutrophilic influx (142.5 ± 12.8 PMNs/HPF) and profound adipocyte depletion ($4.2 \pm 1.1\%$ vs $52.4 \pm 4.1\%$, $p < 0.001$). By Day 10, PMN counts significantly declined (31.4 ± 5.6 cells/HPF, $p < 0.001$), accompanied by a marked surge in mononuclear cells (macrophages: 68.3 ± 7.2 cells/HPF; lymphocytes: 45.2 ± 5.1 cells/HPF), shifting the Neutrophil-to-Mononuclear (N/M) ratio from 3.29 down to 0.24. Digital histomorphometry combined with differential cellular profiling on H&E sections provides a very sensitive and objective dual matrix paradigm for the quantification of the marrow space remodeling during bacterial osteomyelitis.

Open Access

Citation: Ali MB et al. (2026) Histomorphometric and Temporal Evaluation of Bacterial-Induced Mandibular Bone Marrow Inflammation (Osteolyelitis). Dentistry 3000. 1:a001 doi:10.5195/d3000.2026.1596
Received: September 13, 2026
Accepted: September 20, 2026
Published: September 22, 2026

Email: Mustafab.altalqani@uokufa.edu.iq

Introduction

Osteomyelitis of the jaws is a complicated inflammatory disease, caused mainly by pyogenic bacterial invasion and Staphylococcus aureus is the main etiologic pathogen in more than 80% of the clinical cases [1,2]. Unlike appendicular skeleton bones, the mandible possesses distinct anatomical features including a heavy cortical plate, terminal end-artery intraosseous blood supply, and proximity to dental structures, making its intramedullary vascular bed exceptionally susceptible to septic thrombosis, ischemia, and rapid necrosis [3,4].

The main causes of osteomyelitis are odontogenic (dental infection) or traumatic (fracture). Patients with osteomyelitis commonly have experienced a traumatic event such as traumatic tooth extraction, a chronically inflamed carious tooth, a periapical abscess, an infection of adjacent soft tissues, or advanced chronic periodontitis or dental implants [5,6]. *S. aureus* causes the most cases of osteomyelitis due to its frequency, plasticity, and resistance [7-9].

Histopathologic examination of bone specimens coupled with bone culture is considered the gold standard for the diagnosis of osteomyelitis. Despite this, studies have demonstrated histopathologist agreement in the diagnosis of osteomyelitis as low as 30%, largely stemming from a lack of specific definitions and diagnostic criteria [10-12].

Understanding the precise time-course dynamics of these cellular events between the peak acute phase and the subacute transition phase is vital for understanding pathogen-host dynamics [13,14]. This study evaluated the hypothesis that quantitative digital histomorphometry ($H\&E$ + ImageJ analysis) provides precise characterization of cellular density, sinusoidal expansion, adipocyte remodeling, and differential leukocyte dynamics in a rat model of mandibular bacterial bone marrow inflammation.

Material and Methods

Animal Preparation and Experimental Groups

A total of 24 healthy adult male Wistar rats (8–10 weeks old, weighing 220 ± 20 g) were utilized. Animals were housed in standard cages under controlled environmental conditions (22 ± 2°C, 12-hour light/dark cycle) with ad libitum access to food and water [15,16].

Animals were randomly allocated into two main experimental groups ($n = 12$ per group), subdivided by sacrifice time points ($n = 6$ per subgroup):

- Control Group: Received an intraosseous intramedullary injection of $10\ \mu$L sterile phosphate-buffered saline (PBS) [10].
  - Subgroup 1A: Sacrificed at Day 5 ($n = 6$).
  - Subgroup 1B: Sacrificed at Day 10 ($n = 6$).
- Infected Group: Received an intraosseous intramedullary injection of $10\ \mu$L *S. aureus* suspension (1×10^7 CFU/mL) [9,10].
  - Subgroup 2A: Sacrificed at Day 5 ($n = 6$).
  - Subgroup 2B: Sacrificed at Day 10 ($n = 6$).

Surgical Protocol and Infection Induction

Surgical procedures were performed under general anesthesia induced via intraperitoneal administration of ketamine (80 mg/kg) and xylazine (10 mg/kg) [17]. A 1 cm extraoral incision was made along the inferior border of the left mandibular angle. The masseter muscle was elevated to expose the cortical bone [18]. A sub-millimeter cortical defect was created using a round dental bur under continuous cold saline irrigation [19,20]. A 27-gauge needle was inserted directly into the medullary canal to deliver $10\ \mu$L of bacterial suspension or PBS. The defect was sealed with sterile bone wax, and tissues were sutured in layers [21-23].

Tissue Processing and Histology

At days 5 and 10 post-surgery, animals were humanely euthanized via sodium pentobarbital overdose (150 mg/kg IP). Mandibles were harvested, fixed in 10% neutral buffered formalin (NBF) for 24 hours, and decalcified in 14% EDTA (pH 7.2) at 4°C for 4 weeks. Decalcified specimens were paraffin-embedded, longitudinally sectioned at $4\ \mu$m thickness, and stained with Hematoxylin and Eosin (H&E) [24-26].

Digital Histomorphometry and Differential Cellular Analysis

Five non-overlapping high-power fields (HPFs, 40x magnification, field area $= 0.16$ mm^2) per section were randomly selected within the medullary cavity using an Olympus BX53 light microscope. Quantitative image processing was conducted using ImageJ software (v1.53, NIH, USA) [27]. Overall marrow parameters were defined by the total marrow cell density (cells/mm^2), adipocyte area percentage (%), sinusoidal area percentage (%), and semi-quantitative marrowitis score (0–4). Differential inflammatory cell count (cells/HPF) was defined by specific identification and manual counting of polymorphonuclear neutrophils (PMNs), macrophages/monocytes, lymphocytes, and plasma cells based on standard nuclear morphologic criteria. Neutrophil-to-mononuclear (N/M) Ratio was calculated as $\frac{\text{PMNs}}{\text{Macrophages+Lymphocytes+Plasma Cells}}$.

Statistical Analysis

Data were analyzed using GraphPad Prism (v9.0) and presented as Mean $\pm$ Standard Deviation (SD). A Two-Way Analysis of Variance (Two-Way ANOVA) was performed with two independent factors: *Treatment Group* and *Time Point*. Post-hoc comparisons were conducted using Tukey's Multiple Comparisons Test [8]. Statistical significance was set at $p < 0.05$.

Results

Overall Histomorphometry Parameters (Table 1)

A highly significant interaction was observed between infection status and post-inoculation time point across all structural parameters ($p < 0.001$) [8,12].

Differential Inflammatory Cell Profiling (Table 2)

To precisely quantify the immunocellular transition from acute purulent inflammation to chronic mononuclear remodeling, differential cell counts were performed per HPF [15,20,23].

Histopathological Narrative

Control groups (days 5 and 10) maintained physiological bone marrow histology with intact fat vacuoles, normal hematopoietic lineages, and low background inflammatory counts. Infected group at day 5 exhibited acute purulent bone marrow inflammation marked by massive PMN extravasation (142.5 ± 12.8 cells/HPF), sinusoidal dilation (31.8%), and adipocyte collapse (4.2%), yielding a high N/M ratio of 3.29 ± 0.35. Infected group at day 10 demonstrated a significant decline in PMNs (31.4 ± 5.6 cells/HPF, $p < 0.001$) along with a major surge in macrophages (68.3 ± 7.2 cells/HPF) and lymphocytes (45.2 ± 5.1 cells/HPF) [15,22]. This shift dropped the N/M ratio to 0.24 ± 0.05, confirming subacute/chronic immunomodulatory transition.

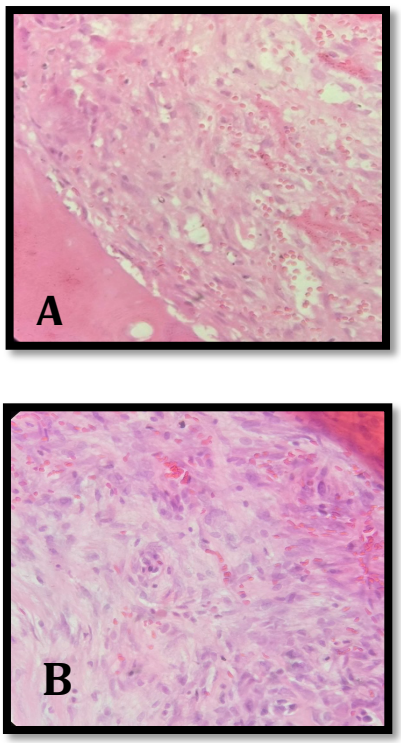

Figure 3. Control 5 day (A), control 10 days (B) both is a normal control bone marrow, showing baseline normocellular hematopoietic tissue and normal architecture without stimulation or reactive changes, and a well-organized interface with the continuous trabecular bone.

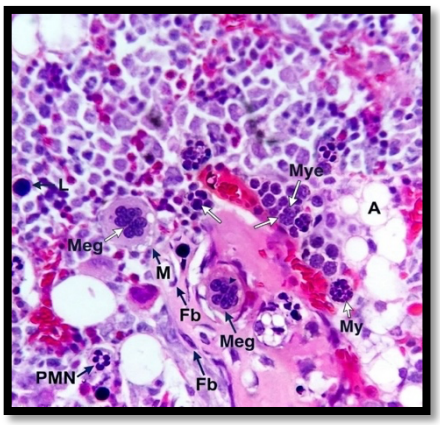

Figure 4. infected group (5 Days) shows marked hypercellularity with active trilineage hematopoiesis (Mye Myeloid precursors, Meg Megakaryocyte), scattered Lymphocytes (L), Neutrophils (PMN), and scarce Adipocytes (A). The stroma exhibits Fibroblasts (Fb), Macrophages (M), and Vascular congestion (C), adjacent to Trabecular bone (TB) undergoing resorption by an Osteoclast (Oc). (H&E stain) 40X.

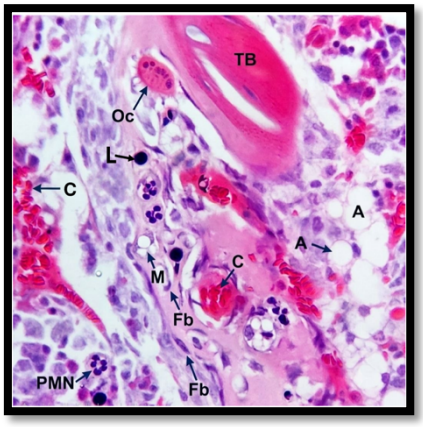

Figure 5. infected group (10 days) remodeling rat bone marrow, displaying prominent Osteoclastic activity (Oc) along the Trabecular bone (TB), active Fibroplasia (Fb), Vascular congestion (C),Adipocytes (A) and scattered inflammatory/hematopoietic cells (PMN Neutrophils, L lymphocyte, M Macrophages). (H&E stain) 40X.

Discussion

The current study provides a high-resolution, quantitative temporal map of the intramedullary environment during the progression of mandibular osteomyelitis (OM). By utilizing digital histomorphometry, we transitioned from subjective descriptions to objective metrics, capturing the rapid immunocellular shifts between the acute (Day 5) and subacute (Day 10) phases of *Staphylococcus aureus* infection.

The Mandibular Microenvironment and Vascular Susceptibility

Our findings demonstrate marked architectural changes in the mandibular marrow within 120 hours following bacterial inoculation. The increased susceptibility of the mandible to osteomyelitis has been attributed, at least in part, to its relatively limited vascular supply and dense cortical architecture, which may compromise tissue perfusion and impair the host response to infection. The mandibular blood supply is predominantly derived from the inferior alveolar artery, while vascular compromise during inflammation may contribute to thrombosis, ischemia, and subsequent bone necrosis [28-30].

Marrow Adipose Tissue (MAT) as an Inflammatory Fuel

One of the most striking findings in our study was the nearly total depletion of marrow adipocytes at day 5 (4.2% vs. 52.4% in controls). Historically regarded largely as an inert filler of the marrow cavity, bone marrow adipose tissue (BMAT) is now recognized as a dynamic and metabolically active component of the marrow microenvironment. Recent studies have demonstrated that marrow adipocytes possess endocrine and paracrine functions and interact with hematopoietic, skeletal, and immune pathways. BMAT-derived adipokines and other signaling mediators may therefore contribute to the regulation of immune homeostasis and inflammatory responses within the bone marrow [31-34].

The Neutrophil-to-Mononuclear (N/M) Ratio: A Temporal Pivot

The marked decline in the N/M ratio from 3.29 at day 5 to 0.24 at day 10 indicates a substantial shift in the cellular composition of the mandibular inflammatory infiltrate, from a PMN-dominant acute response toward a predominantly mononuclear-cell infiltrate. The pronounced accumulation of PMNs at day 5 is consistent with the early innate response to pyogenic bacterial infection. During acute infection, increased neutrophil demand can activate emergency granulopoiesis, a hematopoietic adaptation that accelerates neutrophil production and mobilization from the bone marrow. Recent studies have further demonstrated the involvement of G-CSF-dependent pathways in murine *S. aureus* osteomyelitis, linking neutrophil responses to inflammatory signaling and bone loss [35-37].

By day 10, the marked increase in macrophages (68.3 cells/HPF) and lymphocytes (45.2 cells/HPF) suggests a shift in the cellular composition of the inflammatory infiltrate toward a more mononuclear-dominant response. Recent studies indicate that macrophages play a central role in determining the balance between persistent inflammation and tissue repair during bone infection. In acute bacterial infection, pro-inflammatory M1-like macrophage activity contributes to pathogen clearance, whereas subsequent acquisition of M2-like or pro-resolving phenotypes is associated with inflammatory resolution and tissue repair. In S. aureus-associated osteomyelitis, disruption of this macrophage phenotypic transition may contribute to persistent inflammation, impaired bone repair, and chronic infection [38-41].

Digital Histomorphometry: Overcoming Diagnostic Subjectivity

Our research findings show that using the tool ImageJ to conduct digital image analysis constitutes a replicable method. What does replicable mean? It means that no matter who operates this set of procedures, consistent and stable results can be obtained in the end, and conclusions that diverge drastically will not be reached due to differences in operators. This method not only enables quantitative assessment of tissue morphology—that is, converting the morphological characteristics of tissues into specific numerical values for description, which differs from traditional methods that only rely on the naked eye to assign grades and judge quality—but also compensates for the shortcomings of traditional qualitative histological grading methods. This set of methods can eliminate the subjective bias of manual judgment, objectively calculate the specific values of parameters such as bone marrow cell density and sinus tract area, and also capture structural changes that may not be stably defined by descriptive assessment alone [42].

Clinical Implications and Future Research Directions

These findings serve as a reminder for clinical maxillofacial surgeons: there is a critical golden window for performing interventional therapy on patients, and the efficacy of intervention will be greatly diminished if this period is missed.

Within just five days after injury, patients will experience a large-scale disappearance of adipocytes and a sharp surge in the number of neutrophils. These two distinct changes indicate that the progression of injuries within the bone marrow is far faster than the rate that can typically be captured by conventional X-ray imaging—often, before any abnormalities are detected on X-rays, the injury in the bone marrow has already progressed for a considerable period.

The N/M ratio mentioned herein refers to the ratio of the number of neutrophils to macrophages. A shift in this ratio means that by the tenth day post-injury, the original acute lesion has transitioned into a chronic remodeling phase, and the body enters a long-term process of tissue adjustment.

This study only tracked changes in the first ten days after injury. Future research needs to explore the "third stage" of infection, with a focus on analyzing the association between the early-stage bone marrow remodeling that occurs in this phase and the formation of a sequestrum in the later stage—that is, the formation of small necrotic bone fragments that break away from the body's normal tissue.

In addition, it is feasible to explore the application of AI-powered automatic cell counting technology, which uses artificial intelligence to automatically count cell numbers, to optimize the digital histomorphometric system established in this study, making this method of digitally analyzing tissue morphology more accurate and robust.

Conclusion

1. Intraosseous injection of *S. aureus* in the rat mandible provides a consistent animal model for acute and chronic osteomyelitis.
2. Peak acute purulent inflammation occurs at day 5, characterized by PMN predominance ($N/M\ ratio = 3.29$) and severe adipocyte loss [13,20].

3. Day 10 marks a significant transition to chronic mononuclear infiltration ($N/M\ ratio = 0.24$) and partial fat space recovery.
4. Dual-table digital histomorphometry offers a quantitative, reproducible methodology for evaluating intramedullary inflammatory dynamics.

References

1. Arnold, S. R., Giordano, V., Obremskey, W. T., Schwarz, E. M., Smeltzer, M. S., Veis, D. J., & Cassat, J. E. (2026). Osteomyelitis. *Nature Reviews Disease Primers*, *12*(1), 33.
2. Asnayanti, A., Rathnayake, U., Do, A. D. T., Perera, R., & Alrubaye, A. (2026). Osteomyelitis related lameness across animal species: pathophysiology, etiology, epidemiology and experimental model approaches. *Frontiers in Veterinary Science*, *13*, 1835437.
3. Kumar, M., Mohit, V., Attri, N. C., Fayaz, A., Harleen, K., Rishabh, K., & Gupta, S. (2025). Anterior mandibular osteomyelitis: a narrative review of clinical presentation, diagnosis, and management strategies. *Cureus*, *17*(6).
4. Josse, J., et al. (2015). *Staphylococcus aureus* interaction with bone cells: a review. *PLOS Pathogens*, 11(10), e1005178.
5. López-Carriches, C., Mateos-Moreno, M. V., Taheri, R., Martínez, J. L. Q., & Madrigal-Martínez-Pereda, C. (2025). Chronic Osteomyelitis of the jaw. Osteomyelitis. *Journal of clinical and experimental dentistry*, *17*(3), e324.
6. Castillo, C. A. P., Mousavian, M., Peacock, Z., & Barshak, M. B. (2025). Jaw osteomyelitis. *Infectious Disease Clinics*, *39*(3), 483-500.
7. Song, M., Sun, J., Lv, K., Li, J., Shi, J., & Xu, Y. (2025). A comprehensive review of pathology and treatment of staphylococcus aureus osteomyelitis. *Clinical and Experimental Medicine*, *25*(1), 131.
8. Granata, V., Possetti, V., Parente, R., Bottazzi, B., Inforzato, A., & Sobacchi, C. (2022). The osteoblast secretome in Staphylococcus aureus osteomyelitis. *Frontiers in Immunology*, *13*, 1048505.
9. Tong, E., Dong, X., Ren, Y., Gong, L., Zhao, C., Nie, R., & Meng, X. (2026). Artesunate ameliorates Staphylococcus aureus-induced mandibular osteomyelitis and promotes osteogenic differentiation via NOD2/p65 signaling pathway. International Immunopharmacology, 175, 116472.
10. Weihe, R., Taghlabi, K., Lowrance, M., Reeves, A., Jackson, S. R., Burton, D. C., & El Atrouni, W. (2022, March). Culture yield in the diagnosis of native vertebral osteomyelitis: a single tertiary center retrospective case series with literature review. In *Open Forum Infectious Diseases* (Vol. 9, No. 3, p. ofac026). US: Oxford University Press.
11. Peterlin, A. A., McNally, M., Henriksen, N. L., Blirup-Plum, S. A., Jørgensen, A., Jørgensen, A. I., ... & Jensen, L. K. (2025). Exploring the value of paired microbiology and histology in chronic osteomyelitis and fracture-related infections. *Antibiotics*, *14*(12), 1277.
12. Refaie, S. M., Khan, I. A., & Hashmi, S. Z. A. (2026). Precision diagnosis of bone and joint infections: Integrating pathology, clinical microbiology, molecular diagnostics, and surgical management a systematic review. Genetics and Molecular Research.
13. Martin, V. T., Lin, Y., Wu, H., Yu, B., Guan, D., Wang, J., & Yu, B. (2026). An injectable AsCu-nanocomposite hydrogel breaks the pathological triad of acute osteomyelitis via synergistic bactericidal and macrophage-reprogramming therapy. *Nano Research*.
14. Bhagat, S., Kaur, K., Petronglo, J. R., O'Connor, L., Wang, C., Li, Y., ... & Mbalaviele, G. (2026). Staphylococcus aureus inhibits the NLRP3 inflammasome in macrophages to varying degrees during early and late stages of infection. *Infection and Immunity*, e00200-26.
15. Meroni, G., Tsikopoulos, A., Tsikopoulos, K., Allemanno, F., Martino, P. A., & Soares Filipe, J. F. (2022). A journey into animal models of human osteomyelitis: a review. *Microorganisms*, *10*(6), 1135.
16. Almalki, A. H., Hassan, W. H., Belal, A., Farghali, A., Saleh, R. M., Allah, A. E., ... & Abo El-Ela, F. I. (2023). Exploring the antimicrobial activity of sodium titanate nanotube biomaterials in combating bone infections: an in vitro and in vivo study. *Antibiotics*, *12*(5), 799.
17. Khalel, A. M., & Fadhil, E. (2020). Histological and immunohistochemical study of osteocalcin to evaluate the effect of local application of Symphytum officinale oil on bone healing on rat.
18. Alrashid, H. H. A. (2024). Evaluating Regenerative Potential: Dental Pulp Stem Cells (DPSCs) and OsteoBiol Gen-Os® Scaffold for Enhanced Bone Repair in Rat Mandibular Defects.
19. Sasaki, T., Watanabe, M., Omori, T., & Sasaki, N. (2026). Euthanasia efficacy and plasma biochemical implications of intraperitoneal thiamylal sodium in three rat strains. Journal of Veterinary Medical Science, 88(1), 50-53.
20. Hassan, M. A. A., Khalel, A. M., & Ajwad, A. A. (2024). Histological and Histomorphometric illustration the endochondral ossification of the mandibular angle defect repair in rats after oral stimulation with bisphosphonate treatment (an in vivo study).
21. Varoga, D., Tohidnezhad, M., Paulsen, F., Wruck, C. J., Brandenburg, L., Mentlein, R., ... & Pufe, T. (2008). The role of human β-defensin-2 in bone. Journal of anatomy, 213(6), 749-757.
22. Odekerken, J. C., Arts, J. J., Surtel, D. A., Walenkamp, G. H., & Welting, T. J. (2013). A rabbit osteomyelitis model for the longitudinal assessment of early post-operative implant infections. Journal of Orthopaedic Surgery and Research, 8(1), 38.
23. Giavaresi, G., Meani, E., Sartori, M., Ferrari, A., Bellini, D., Sacchetta, A. C., ... & Romanò, C. L. (2014). Efficacy of antibacterial-loaded coating in an in vivo model of acutely highly contaminated implant. International orthopaedics, 38(7), 1505-1512.
24. Balto, K., Sasaki, H., & Stashenko, P. (2001). Interleukin-6 deficiency increases inflammatory bone destruction. Infection and immunity, 69(2), 744-750.
25. Alemi, A. S., Mazur, C. M., Fowler, T. W., Woo, J. J., Knott, P. D., & Alliston, T. (2018). Glucocorticoids cause mandibular bone fragility and suppress osteocyte perilacunar-canalicular remodeling. Bone Reports, 9, 145-153.
26. Austah, O. N., Lillis, K. V., Akopian, A. N., Harris, S. E., Grinceviciute, R., & Diogenes, A. (2022). Trigeminal neurons control immune-bone cell interaction and metabolism in apical periodontitis. *Cellular and Molecular Life Sciences*, *79*(6), 330.
27. Khalel, A. M., Ibrahim, S. M., & Hassan, M. A. A. (2026). Histological analysis of periodontal tissues in patients with autoimmune diseases: a comparative cross-sectional study of inflammatory cell infiltration and epithelial barrier function. *BMC Oral Health*, *26*(1), 741.
28. Kumar, M., Mohit, V., Attri, N. C., Fayaz, A., Harleen, K., Rishabh, K., & Gupta, S. (2025). Anterior mandibular osteomyelitis: a narrative review of clinical presentation, diagnosis, and management strategies. Cureus, 17(6).
29. Xie, Q., Jiang, X., & Huang, X. (2024). Distraction osteogenesis application in bone defect caused by osteomyelitis following mandibular fracture surgery: a case report and literature review. BMC Musculoskeletal Disorders, 25(1), 813.
30. Kawasaki, M., Shimamoto, H., Nishimura, D. A., Yamao, N., Takagawa, N., Uchimoto, Y., ... & Murakami, S. (2025). The usefulness of different imaging modalities in mandibular osteonecrosis and osteomyelitis diagnosis. Scientific Reports, 15(1), 12272.
31. Zhang, X., Tian, L., Majumdar, A., & Scheller, E. L. (2024). Function and regulation of bone marrow adipose tissue in health and disease: state of the field and clinical considerations. *Comprehensive Physiology*, *14*(3), 5521-5579.
32. Marinelli Busilacchi, E., Morsia, E., & Poloni, A. (2024). Bone marrow adipose tissue. Cells, 13(9), 724.

33. Rosen, C. J., & Horowitz, M. C. (2023). Nutrient regulation of bone marrow adipose tissue: skeletal implications of weight loss. *Nature Reviews Endocrinology*, *19*(11), 626-638.
34. Li, Z., & Rosen, C. J. (2023). The multifaceted roles of bone marrow adipocytes in bone and hematopoietic homeostasis. *The Journal of Clinical Endocrinology & Metabolism*, *108*(12), e1465-e1472.
35. Swann, J. W., Olson, O. C., & Passegué, E. (2024). Made to order: emergency myelopoiesis and demand-adapted innate immune cell production. *Nature Reviews Immunology*, *24*(8), 596-613.
36. Paudel, S., Ghimire, L., Jin, L., Jeansonne, D., & Jeyaseelan, S. (2022). Regulation of emergency granulopoiesis during infection. *Frontiers in immunology*, *13*, 961601.
37. Song, M., Deng, M., Peng, Z., Dai, F., Wang, Y., Shu, W., ... & Yu, B. (2024). Granulocyte colony-stimulating factor mediates bone loss via the activation of IL-1β/JNK signaling pathway in murine Staphylococcus aureus-induced osteomyelitis. *International immunopharmacology*, *141*, 112959.
38. Lathram, W. A., & Radka, C. D. (2025). Intracellular survival of Staphylococcus aureus in macrophages during osteomyelitis. *Virulence*, *16*(1), 2553789.
39. Li, J., Zhang, L., Peng, J., Zhao, C., Li, W., Yu, Y., ... & Peng, J. (2025). Mitochondrial metabolic regulation of macrophage polarization in osteomyelitis and other orthopedic disorders: mechanisms and therapeutic opportunities. *Frontiers in Cell and Developmental Biology*, *13*, 1604320.
40. Dai, Y., Yi, X., Huang, Y., Qian, K., Huang, L., Hu, J., & Liu, Y. (2024). miR-345-3p modulates M1/M2 macrophage polarization to inhibit inflammation in bone infection via targeting MAP3K1 and NF-κB pathway. The Journal of Immunology, 212(5), 844-854.
41. Zhao, S. J., Liu, H., Chen, J., Qian, D. F., Kong, F. Q., Jie, J., ... & Fan, J. (2020). Macrophage GIT1 contributes to bone regeneration by regulating inflammatory responses in an ERK/NRF2-dependent way. *Journal of Bone and Mineral Research*, *35*(10), 2015-2031.
42. Azam, A. S., Tsang, Y. W., Thirlwall, J., Kimani, P. K., Sah, S., Gopalakrishnan, K., ... & Snead, D. R. (2024). Digital pathology for reporting histopathology samples, including cancer screening samples–definitive evidence from a multisite study. *Histopathology*, *84*(5), 847-862.

Table 1. Overall histomorphometry parameters of mandibular marrow architecture.

Histomorphometry Parameter	Control Day 5 (n=6)	Infected Day 5 (n=6)	Control Day 10 (n=6)	Infected Day 10 (n=6)	p-value (ANOVA)
Marrow Cell Density (cells/mm^2)	$4{,}205 \pm 310$	$8{,}900 \pm 620^{*\#}$	$4{,}310 \pm 280$	$6{,}450 \pm 490^{*\dagger}$	$p < 0.001$
Adipocyte Area (%)	$52.4 \pm 4.1\%$	$4.2 \pm 1.1\%^{*\#}$	$50.8 \pm 3.8\%$	$18.6 \pm 2.9\%^{*\dagger}$	$p < 0.001$
Sinusoidal Area (%)	$8.5 \pm 1.2\%$	$31.8 \pm 3.4\%^{*\#}$	$8.9 \pm 1.0\%$	$19.4 \pm 2.1\%^{*\dagger}$	$p < 0.001$
Histological Marrow inflammation Score (0–4)	0.17 ± 0.40	$3.83 \pm 0.40^{*\#}$	0.20 ± 0.40	$2.33 \pm 0.50^{*\dagger}$	$p < 0.001$

** Significant vs corresponding Control ($p < 0.001$).*
 # Significant vs Infected Day 10 ($p < 0.01$).
\† Significant vs Infected Day 5 ($p < 0.01$).

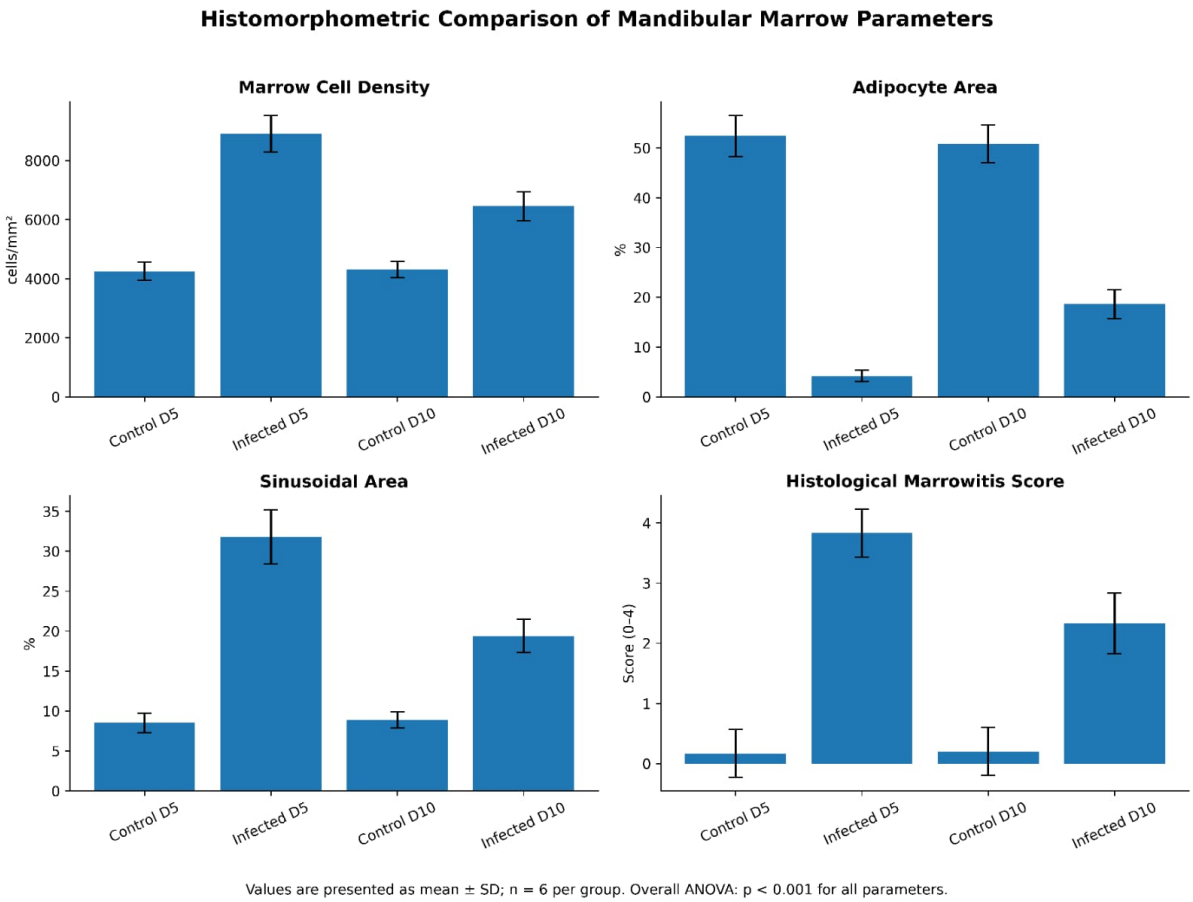

Figure 1. Quantitative histomorphometry analysis of mandibular marrow parameters. Comparison of (A) marrow cell density, (B) adipocyte area, (C) sinusoidal area, and (D) histological marrowitis score between Control and Infected groups at Day 5 and Day 10. Bars represent Mean ± SD ($n = 6$ per group). Overall ANOVA indicates $p < 0.001$ for all parameters.

Table 2. Differential inflammatory cell counts per high-power field (HPF at 40x).

Inflammatory Cell Lineage (cells/HPF)	Control Day 5 (n=6)	Infected Day 5 (n=6)	Control Day 10 (n=6)	Infected Day 10 (n=6)	p-value (ANOVA)
Polymorphonuclear Neutrophils (PMNs)	3.2 ± 1.1	$142.5 \pm 12.8^{*\#}$	3.0 ± 1.2	$31.4 \pm 5.6^{*\dagger}$	$p < 0.001$
Macrophages / Monocytes	8.4 ± 1.8	$22.1 \pm 3.4^{*\#}$	8.1 ± 1.5	$68.3 \pm 7.2^{*\dagger}$	$p < 0.001$
Lymphocytes	12.1 ± 2.3	$18.4 \pm 2.9^{*\#}$	11.8 ± 2.1	$45.2 \pm 5.1^{*\dagger}$	$p < 0.001$
Plasma Cells	1.5 ± 0.8	2.8 ± 1.1	1.4 ± 0.7	$16.7 \pm 2.4^{*\dagger}$	$p < 0.001$
Neutrophil-to-Mononuclear Ratio (N/M Ratio)	0.15 ± 0.04	$3.29 \pm 0.35^{*\#}$	0.14 ± 0.03	$0.24 \pm 0.05^{*\dagger}$	$p < 0.001$

** Significant vs corresponding Control ($p < 0.001$).*
 # Significant vs Infected Day 10 ($p < 0.01$).
\† Significant vs Infected Day 5 ($p < 0.01$).

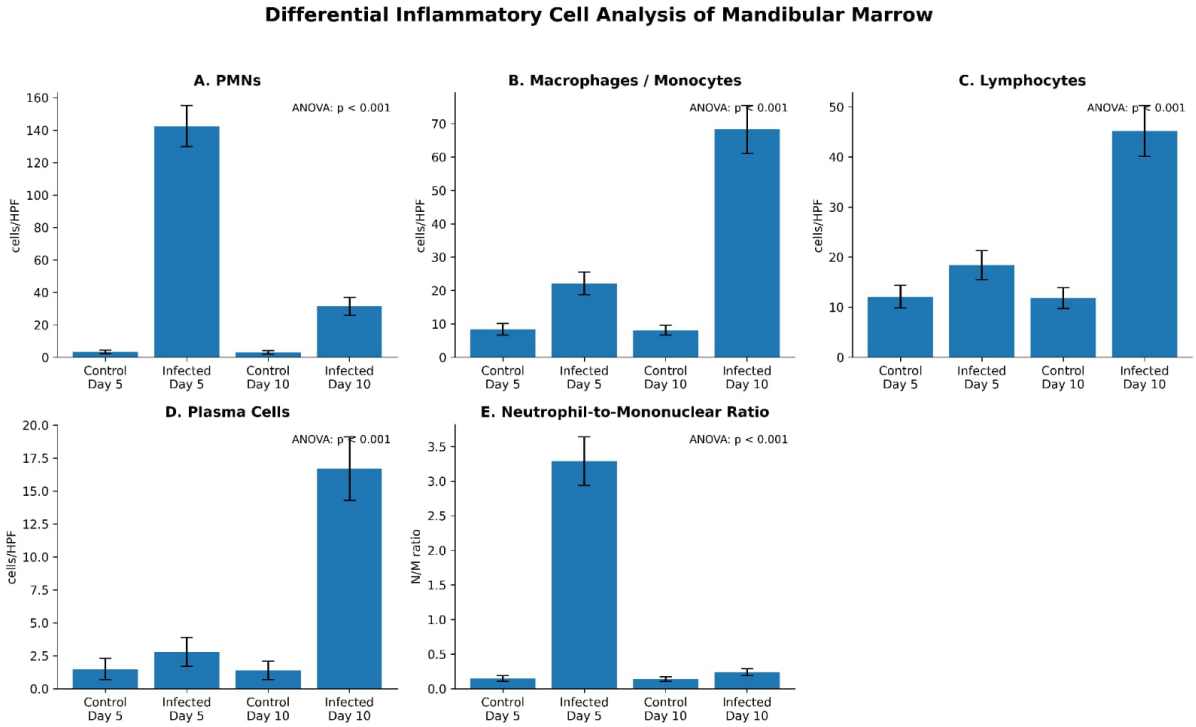

Figure 2. Quantitative analysis of inflammatory cell populations and the neutrophil-to-mononuclear (N/M) ratio in mandibular bone marrow following Staphylococcus aureus infection. Values are presented as mean ± SD (n = 6); $p < 0.001$ by one-way ANOVA.